CHEMISTRY OF MATERIALS

ARTICLE

pubs.acs.org/cm

Star-Shaped Glycosylated Conjugated Oligomer for Two-Photon Fluorescence Imaging of Live Cells

Guan Wang,[†,‡] Kan-Yi Pu,[†] Xinhai Zhang,[§] Kai Li,[†] Long Wang,[†] Liping Cai,[†] Dan Ding,[†] Yee-Hing Lai,[*,‡] and Bin Liu[*,†,§]

[†]Department of Chemical and Biomolecular Engineering, 4 Engineering Drive 4, National University of Singapore, Singapore 117576

[‡]Department of Chemistry, 3 Science Drive 3, National University of Singapore, Singapore 117543

[§]Institute of Materials Research and Engineering, Singapore 117602

Supporting Information

ABSTRACT: A star-shaped glycosylated conjugated oligomer, 4,4′,4″-tris(4-(2-(4-(benzo[d]thiazol-2-yl)phenyl)-9,9′-bis(6-thiol-β-D-glucose)-hexyl)-fluoren-7-yl)phenylamine (TFBS), is synthesized for two-photon fluorescence imaging of live cells. The high density of hydrophilic sugar side groups induces self-assembly of TFBS into nanoparticles in water with an average diameter of 61 nm. Because of the self-assembled nanostructure, TFBS has a higher quantum yield in water (Φ = 0.10), compared to its cationic counterpart, 4,4′,4″-tris(4-(2-(4-(benzo[d]thiazol-2-yl)phenyl)-9,9′-bis(6-*N*,*N*,*N*-trimethylammonium)-hexyl)-fluoren-7-yl)phenylamine (TFBC) (Φ = 0.03). In addition, TFBS has a large TPA cross section (δ_{max}) of ~1200 GM at 740 nm in aqueous media, which is significantly higher than that for TFBC. TFBS can be effectively internalized by the human cervical cancer cell line and accumulates in the cytoplasm, allowing for live cell two-photon fluorescence imaging upon 800-nm excitation. TFBS has also shown low cytotoxicity, which is essential for in vitro and in vivo cellular imaging and other clinical applications. This study demonstrates the significant advantages of glycosylation in molecular engineering of water-soluble fluorescent molecules for two-photon fluorescence imaging applications.

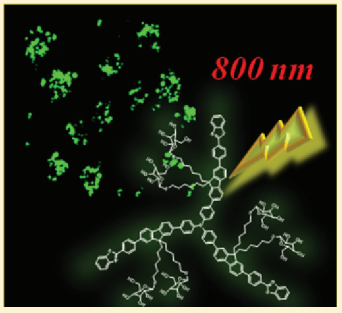

KEYWORDS: star-shaped, water-soluble conjugated oligomer, two-photon fluorescence imaging, live cells, glucose

INTRODUCTION

The development of organic materials with large two-photon absorption (TPA) cross sections (δ) in the near-infrared (NIR) regions (700−1000 nm) has attracted intensive attention in the past two decades, because of their vital applications in three-dimensional (3D) optical data storage, optical power limiting, two-photon microscopy (TPM), and photo dynamic therapy.[1−3] TPM is a powerful technique for noninvasive live cell imaging,[4] because the NIR excitation enables deeper penetration, less photo bleaching, and higher spatial resolution, compared to that for one-photon microscopy (OPM).[5] To obtain a high signal-to-noise ratio in TPM, materials with large TPA action cross sections (defined as $\eta\delta$, where η is the fluorescence quantum yield) are essential. The majority of currently used fluorescent imaging reagents are mainly designed for OPM and are not ideal for TPM, which is characterized by small δ values and low brightness.[6]

Dipolar or quadrupolar models with donor−bridge−donor (D-π-D), donor−bridge−acceptor (D-π-A), and donor−acceptor−donor (D-A-D) architectures have been proven effective in yielding large δ values.[1−3] In comparison with their linear counterparts, multibranched octupolar chromophores are more promising to yield large δ values, because of the excitonic coupling between each branch.[7] By taking this advantage, several octupolar TPA chromophores have been designed and synthesized. Although large δ values of more than ~2000 GM have been obtained among these chromophores,[7−12] they are only soluble in organic solvents, which make them unsuitable for TPM imaging or other biological applications.

Water-soluble π-conjugated TPA molecules generally show significantly decreased δ in water, relative to that for their neutral counterparts in organic solvents.[13] In addition, their η value in water is also low, because of fierce interaction between polar water molecules and chromophores in their excited states through nonradiative decay.[14] Until now, very limited efforts have been made to address these problems. Bazan et al. have reported that the addition of sodium odecyl sulfate (SDS) surfactant into water-soluble paracyclophane chromophores could increase the δ and η values, because of micelle formation.[13] Similarly, Jen et al.[12] reported that the encapsulation of TPA fluorophores with an amphiphilic block copolymer, poly(methacrylic acid)-*block*-polystyrene (PMAA-*b*-PS), led to increased δ values of the fluorophore in micelles. The micellization-enhanced TPA cross sections are associated with the incorporation of optically active units within the hydrophobic microenvironment in the interior of micelles.

On the other hand, glycolipids and carbohydrate compounds have been reported to self-assemble into regular layers or spherical micelles in aqueous media.[15] It occurs to us that the attachment

Received: May 16, 2011
Revised: September 1, 2011
Published: September 26, 2011

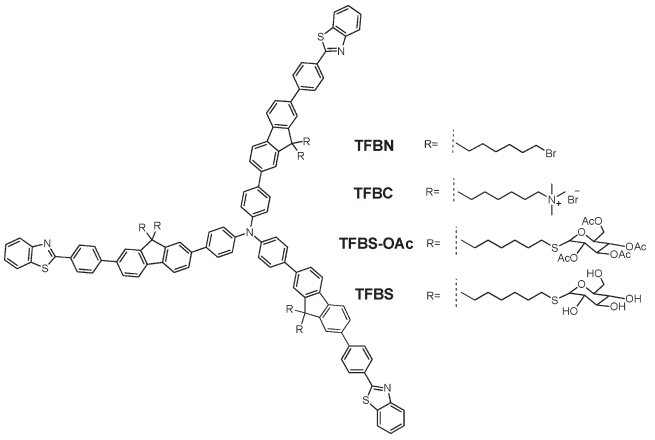

Figure 1. Chemical structures of TFBN, TFBC, TFBS-OAc, and TFBS.

of glycose groups could be an effective strategy to develop amphiphilic multibranched conjugated molecules with intrinsic self-assembly properties. Unlike the micelle-assisted systems, this molecular design could integrate the hydrophilic terminals and the backbone to yield robust water-soluble TPA materials for two-photon fluorescence imaging. Although several examples of metal complexes have been developed as probes for two-photon fluorescence imaging of live cells,[16−18] these probes are generally highly toxic to cells and possess small δ values (<100 GM). To the best of our knowledge, there are only a limited number of organic fluorophores designed for two-photon imaging of live cells,[19−22] of which the δ values are also very small (<20 GM).

In this contribution, we report a star-shaped glycosylated conjugated oligomer (TFBS) with high TPA cross sections in aqueous solution for two-photon fluorescence imaging of live cells. A cationic conjugated oligomer (TFBC) as the counterpart of TFBS has also been synthesized to investigate how the terminal group of conjugated oligomers affects their self-assembly behavior in aqueous media and, in turn, determines their linear and nonlinear properties. The chemical structures of TFBC and TFBS are shown in Figure 1. To fulfill a good charge transfer feature from center to terminals, triphenylamine was used as the donor, while fluorene was chosen as the bridge, with phenylbenzo[d]thiazole as the terminal acceptor.[23]

EXPERIMENTAL SECTION

Materials and Instruments. Chemicals and reagents were purchased from Aldrich Chemical Co. unless otherwise stated. NMR spectra were collected on a Bruker Model ACF 300 or Model AMX 500 spectrometer with chloroform-*d* as the solvent (unless otherwise stated) and tetramethylsilane as the internal standard. Elemental analysis were carried out by the Microanalysis Laboratory of the National University of Singapore. UV−vis spectra were recorded on a Shimadzu Model UV-1700 spectrometer. Fluorescence measurements were carried out on a Perkin−Elmer LS-55 instrument equipped with a xenon-lamp excitation source and a Hamamatsu (Japan) 928 photomultiplier tube (PMT), using 90^o angle detection for solution samples. Quantum yields were measured using quinine sulfate as the standard, with a quantum yield of 55% in H_2SO_4 (0.1 M).

Synthesis of 2-(4-bromophenyl)benzo[d]thiazole (1). A mixture of 4-bromobenzaldehyde (3.7 g, 20 mmol), 2-aminothiophenol (2.5 g, 20 mmol), and *N*-methyl-2-pyrrolidone (NMP) (30 mL) was heated in an oil bath at 110 °C for 72 h, which was then poured into 1:1 ethanol/water. The precipitates were collected, recrystallized from ethanol to afford **1** as yellow needle-shaped crystals (2.8 g, 80%). ^{1}H NMR ($CDCl_3$, 500 MHz, ppm): δ 8.07 (d, 1H, J = 8.2 Hz), 7.94 (d, 2H, J = 8.5 Hz), 7.89 (d, 1H, J = 7.9 Hz), 7.61 (d, 2H, J = 8.6 Hz), 7.50 (t, 1H, J = 7.7 Hz), 7.39 (t, 1H, J = 7.6 Hz). ^{13}C NMR ($CDCl_3$, 125 MHz, ppm): δ 166.68, 154.08, 135.06, 132.55, 132.23, 128.91, 126.51, 125.46, 125.44, 123.34, 121.67. HRMS (EI, m/z): calcd 288.9561 (for $C_{13}H_8N_1{}^{79}Br_1{}^{32}S_1$) and 290.9540 (for $C_{13}H_8N_1{}^{81}Br_1{}^{32}S_1$); found: 288.9566, 290.9548.

Synthesis of 2-(4-(4,4,5,5-tetramethyl-1,3,2-dioxaborolan-2-yl)phenyl)benzo[d]thiazole (2). 2-(4-Bromophenyl)benzo[d]-thiazole (2.4 g, 8.3 mmol), bis(pinacolato)diborane (2.5 g, 10 mmol), KOAc (2.9 g, 29 mmol), and dioxane (60 mL) were mixed together in a 100-mL flask. After degassing, [Pd(dppf)Cl_2] (250 mg, dppf = 1,1′-bis(diphenylphosphanyl)ferrocene) was added. The reaction mixture was kept at 85 °C overnight, which was then cooled to room temperature. After the organic solvent was removed, the residual was dissolved in dichloromethane and washed with water. After drying with $MgSO_4$, the solvent was distilled out. The crude product was purified by chromatography using ethylacetate/hexanes (1:9) as eluent to give **2** as a white solid (2.4 g, 86%). ^{1}H NMR ($CDCl_3$, 500 MHz, ppm): δ 8.02 (dd, 4H, J = 8.1 Hz, J = 79.7 Hz), 7.99 (dd, 2H, J = 8.0 Hz, J = 95.8 Hz), 7.49 (t, 1H, J = 7.7 Hz), 7.38 (t, 1H, J = 7.6 Hz), 1.37 (s, 12H). ^{13}C NMR ($CDCl_3$, 125 MHz, ppm): δ 167.97, 154.18, 135.87, 135.39, 135.16, 126.69, 126.38, 125.33, 123.36, 121.65, 84.11, 25.04. HRMS (EI, m/z): calcd for $C_{19}H_{20}O_2N_1{}^{11}B_1{}^{32}S_1$, 337.1308; found, 337.1312.

Synthesis of 2-(4-(2-Bromo-9,9′-bis(6-bromohexyl)-fluoren-7-yl)phenyl)benzo[d]thiazole (4). 2-(4-(4,4,5,5-Tetramethyl-1,3,2-dioxaborolan-2-yl)phenyl)benzo[d]thiazole (216 mg, 0.64 mmol) and 2,7-dibromo-9,9′-bis(6-bromohexyl)fluorene (1.3 g, 1.9 mmol), $Pd(PPh_3)_4$ (37 mg, 0.02 mmol), tetrabutylammonium bromide (cat. amount), toluene (8 mL), 2 M Na_2CO_3 aqueous solution (1 mL) were mixed together in a 100-mL round-bottom flask, and the mixture was then degassed. The reaction was kept at 100 ^{o}C overnight before it was cooled to room temperature. Dichloromethane was added for extraction, and the organic layer was washed successively with brine and water, and then dried with $MgSO_4$. After solvent removal, the crude product was purified with gradient column chromatography using ethyl acetate/hexane (1:100) and then ethyl acetate/hexane (1:9) to afford **4** as a white solid (166 mg, 50%). ^{1}H NMR ($CDCl_3$, 500 MHz, ppm): δ 8.21 (d, 2H, J = 8.3 Hz), 8.11 (d, 1H, J = 8.1 Hz), 7.93 (d, 1H, J = 7.9 Hz), 7.80 (d, 2H, J = 8.3 Hz), 7.76 (d, 1H, J = 7.9 Hz), 7.66 (dd, 1H, J = 1.4 Hz, J = 7.9 Hz), 7.60 (m, 2H), 7.51 (m, 4H), 7.41 (t, 1H, J = 7.6 Hz), 3.28 (t, 4H, J = 6.8 Hz), 2.06−1.96 (m, 4H), 1.70−1.64 (m, 4H), 1.25−1.07 (m, 8H), 0.70−0.64 (m, 4H). ^{13}C NMR ($CDCl_3$, 125 MHz, ppm): δ 167.35, 154.08, 152.78, 150.71, 143.52, 139.83, 139.43, 139.18, 134.90, 132.34, 130.10, 127.88, 127.45, 126.23, 126.00, 125.07, 123.06, 121.49, 121.27, 121.20, 121.04, 120.20, 55.30, 39.93, 33.76, 32.46, 28.82, 27.59, 23.43. HRMS (EI, m/z): calcd 777.0275 (for $C_{38}H_{38}N_1{}^{79}Br_3{}^{32}S_1$), 781.0234 (for $C_{38}H_{38}N_1{}^{79}Br_1{}^{81}Br_2{}^{32}S_1$), and 779.0255 (for $C_{38}H_{38}N_1{}^{79}Br_2{}^{81}Br_1{}^{32}S_1$); found: 777.0255, 781.0214, 779.0223.

Synthesis of 4,4′,4″-Tris(pinacolatoborane)phenylamine (5). Tris(4-bromophenyl)amine (1.93 g, 4 mmol), bis(pinacolato)diborane (3.75 g, 15 mmol), KOAc (7.0 g, 70 mmol), and dioxane (60 mL) were mixed together in a 100-mL flask. After degassing, [Pd(dppf)Cl_2] (0.5 g, dppf = 1,1′-bis(diphenylphosphanyl)ferrocene) was added. The reaction mixture was kept at 85 °C overnight before it was cooled to room temperature. The organic solvent was removed, and the residual was dissolved in dichloromethane and washed with water. After drying the organic layer with $MgSO_4$, the solvent was removed. The crude product was purified by flash chromatography, using hexane and dichloromethane (2:1) as an eluent, to give **5** as a white solid (4.2 g, 59%). ^{1}H NMR ($CDCl_3$, 500 MHz, ppm): δ 7.68 (d, 6H, J = 8.3 Hz), 7.07 (d, 6H, J = 8.4 Hz), 1.34 (s, 36H). ^{13}C NMR ($CDCl_3$, 125 MHz, ppm): δ 149.80, 135.94, 123.50, 83.70, 24.90.

dx.doi.org/10.1021/cm201377u |*Chem. Mater.* 2011, 23, 4428–4434

Synthesis of 4,4′,4″-Tris(4-(2-(4-(benzo[d]thiazol-2-yl)-phenyl)-9,9′-bis(6-bromohexyl)-fluoren-7-yl)phenylamine (TFBN). 2-(4-(2-Bromo-9,9′-bis(6-bromohexyl)-fluoren-7-yl)phenyl)-benzo[d]thiazole (395 mg, 0.5 mmol) and 4,4′,4″-tris(pinacolatoborane)-phenylamine (88 mg, 0.14 mmol), $Pd(PPh_3)_4$ (37 mg, 3% mmol), tetrabutylammonium bromide (cat. amount), toluene (5 mL), 2 M Na_2CO_3 aqueous solution (1 mL) were mixed together in a 50-mL Schlenk flask, and the mixture was degassed. The reaction was kept at 100 °C for 48 h before it was cooled to room temperature. Dichloromethane was added for extraction; the organic layer was washed successively with brine and water, and then dried with $MgSO_4$. After the solvent was removed under reduced pressure, the crude product was purified by gradient column chromatography, using toluene/hexanes (5:1), followed by toluene to afford TFBN as a yellowish green solid (60 mg, 18%). ^{1}H NMR ($CDCl_3$, 500 MHz, ppm): δ 8.21 (d, 6H, J = 8.0 Hz), 8.11 (d, 3H, J = 8.0 Hz), 7.93 (d, 3H, J = 7.5 Hz), 7.83 (m, 12H), 7.65 (m, 18H), 7.52 (t, 3H, J = 7.5 Hz), 7.41 (d, 3H, J = 7.5 Hz), 7.34 (d, 6H, J = 8.0 Hz), 3.28 (t, 12H, J = 6.8 Hz), 2.11−2.08 (m,12H), 1.69−1.65 (m,12H), 1.24−1.10 (m, 24H), 0.89−0.77 (m, 12H). ^{13}C NMR ($CDCl_3$, 125 MHz, ppm): δ 151.51, 146.84, 144.07, 140.92, 139.80, 139.64, 138.92, 135.99, 135.10, 132.42, 129.07, 128.26, 128.09, 128.03, 127.67, 126.43, 126.32, 125.87, 125.34, 125.26, 124.56, 123.24, 121.67, 121.29, 120.92, 120.38, 120.28, 55.30, 40.35, 34.00, 32.67, 29.10, 27.80, 23.69. MS (MALDI-TOF, m/z): cald for $C_{132}H_{126}Br_6N_4S_3$, 2344.4; found, 2344.3.

Synthesis of 4,4′,4″-Tris(4-(2-(4-(benzo[d]thiazol-2-yl)-phenyl)-9,9′-bis(6-*N*,*N*,*N*-trimethylammonium)-hexyl)-fluoren-7-yl)phenylamine (TFBC). Trimethylamine (2 mL) was added dropwise to a solution of TFBN (30 mg) in THF (5 mL) at −78 °C. The mixture was stirred for 12 h and then allowed to warm to room temperature. The precipitate was redissolved via the addition of methanol (5 mL). After the mixture was cooled to −78 °C, additional trimethylamine (2 mL) was added, and the mixture was stirred at room temperature for 24 h. After solvent removal, acetone was added to precipitate the quaternized salt TFBC as yellow powders (27 mg, 86%). ^{1}H NMR (MeOD, 500 MHz, ppm): δ 8.11−7.25 (m, 18H), 3.19 (m, 4H), 3.02 (s, 18H), 2.20 (m, 4H), 1.53 (m, 4H), 1.15 (m, 8H), 0.76 (m, 4H). ^{13}C NMR (MeOD, 125 MHz, ppm): δ 167.86, 153.84, 146.83, 141.05, 139.56, 134.72, 132.04, 127.87, 127.75, 127.25, 126.49, 125.98, 125.40, 124.48, 122.52, 121.66, 121.02, 120.51, 66.27, 55.37, 52.14, 39.47, 28.83, 25.37, 23.53, 22.29. MS (MALDI-TOF, m/z): $[M - 2Br]^+$ cald for $C_{150}H_{180}Br_4N_{10}S_3$, 2538.0; found, 2537.8.

Synthesis of 4,4′,4″-Tris(4-(2-(4-(benzo[d]thiazol-2-yl)-phenyl)-9,9′-bis(6-thiol-β-D-glucose tetraacetate)-hexyl)-fluoren-7-yl)phenylamine (TFBS-OAc). TFBN (30 mg, 0.013 mmol), 1-thiol-β-D-glucose tetraacetate (45 mg, 0.123 mmol), and potassium carbonate (130 mg, 1.23 mmol) were placed in a 25-mL round-bottom flask under nitrogen atmosphere. Degassed THF (7 mL) was added to the reaction flask, and the mixture was stirred at room temperature for 2 days. After solvent removal, the residue was dissolved in dichloromethane (15 mL), washed with water, and dried over anhydrous $MgSO_4$. After solvent removal, the crude product was purified by column chromatography on silica gel first with hexane/EtOAc (1:1) to remove excess glucose tetraacetate, which was followed by hexane/EtOAc (1:2) to give the target compound as yellow solid after precipitation in 20 mL of methanol (35 mg, 67%). ^{1}H NMR ($CDCl_3$, 500 MHz, ppm): δ 8.22 (d, 6H, J = 8 Hz), 8.11 (d, 3H, J = 8 Hz), 7.94 (d, 3H, J = 8 Hz), 7.84 (m, 12H), 7.67 (m, 18H), 7.52 (t, 3H, J = 8 Hz), 7.41 (t, 3H, J = 7.5 Hz), 7.33 (d, 6H, J = 8.5 Hz), 5.17 (m, 6H), 5.03 (t, 6H, J = 10 Hz), 4.97 (t, 6H, J = 9.5 Hz), 4.39 (m, 6H), 4.20 (m, 6H), 4.07 (m, 6H), 3.64 (m, 6H), 2.57 (m, 12H), 2.09 (m, 84H), 1.70 (m, 12H), 1.18 (m, 24H), 0.73 (m, 12H). ^{13}C NMR ($CDCl_3$, 125 MHz, ppm): δ 170.16, 169.38, 169.32, 167.71, 154.22, 151.51, 146.79, 144.07, 140.91, 139.77, 138.86, 135.07, 132.39, 128.09, 127.99, 127.66, 126.42, 125.25, 124.50, 123.21, 120.24, 83.57, 83.54, 75.80, 73.89, 69.88, 68.33, 62.12, 55.32, 40.52, 32.63, 29.88, 29.57, 29.46, 28.47, 23.78, 20.71, 20.68, 20.61, 20.58.

Synthesis of 4,4′,4″-Tris(4-(2-(4-(benzo[d]thiazol-2-yl)-phenyl)-9,9′-bis(6-thiol-β-D-glucose)-hexyl)-fluoren-7-yl)-phenylamine (TFBS). TFBS-OAc (30 mg, 0.007 mmol) was dissolved in 2 mL of dry dichloromethane and 4 mL of anhydrous methanol under nitrogen, 0.3 mL of 0.5 M NaOMe in methanol was subsequently added into the solution. The resulting mixture was allowed to react overnight under vigorous stirring at room temperature. After removing the solvent under reduced pressure, water was added to the residue, and the solution was dialyzed against Mill-Q water for 12 h before it was lyophilized to give TFBS as yellow solid (21 mg, 93%). ^{1}H NMR (DMSO, 500 MHz, ppm): δ 8.22−7.27 (m, 18H), 4.98 (m, 4H), 4.39 (m, 2H), 4.16 (m, 2H), 3.61 (m, 2H), 3.36 (m, 2H), 3.05 (m, 4H), 2.17 (m, 4H), 1.34 (m, 16H), 0.64 (m, 4H). ^{13}C NMR (DMSO, 125 MHz, ppm): δ 167.47, 154.17, 151.92, 146.75, 143.69, 141.03, 138.26, 134.97, 132.13, 128.32, 128.10, 127.19, 126.01, 124.73, 123.36, 122.84, 121.01, 85.51, 81.37, 78.65, 73.53, 70.48, 61.65, 56.51, 39.85, 39.69, 39.52, 29.70, 28.58, 19.03. MS (MALDI-TOF, m/z): $[M+H]^+$ cald for $C_{168}H_{12}N_4O_{30}S_9$, 3034.1; found, 3034.1.

Cell Culture and Incubation. Hela cells and NIH-3T3 fibroblast cells were cultured in Dulbecco's Modified Eagle Medium (DMEM) medium containing 10% fetal bovine serum and 1% penicillin−streptomycin at 37 ^{o}C in a humidified environment containing 5% CO_2. Before experiments, the cells were precultured until confluence was reached.

Cell Viability. MTT assays were performed to assess the metabolic activity of NIH-3T3 fibroblast cells. NIH-3T3 cells were seeded in 96-well plates (Costar, Vernon Hills, IL, USA) at an intensity of 2×10^4 cells/mL. After 48 h of incubation, the medium was replaced by TFBS solutions at the concentrations of 0.5 and 1 μM, and the cells were then incubated for 24, 48, and 72 h, respectively. After the designated time intervals, the wells were washed twice with 1× PBS buffer and freshly prepared MTT (100 μL, 0.5 mg/mL) solution in culture medium was added into each well. The MTT medium solution was carefully removed after 3 h of incubation in the incubator.

Isopropanol (100 μL) was then added into each well and the plate was gently shaken for 10 min at room temperature to dissolve all the precipitate formed. The absorbance of MTT at 570 nm was monitored by the microplate reader (Genios Tecan). Cell viability was expressed by the ratio of the absorbance of the cells incubated with TFBS solutions to that of the cells incubated with culture medium only.

Two-Photon Fluorescence Imaging. Hela cells were cultured in chamber (LAB-TEK, Chambered Coverglass System) at 37 °C for qualitative study. After 80% confluence, the medium was removed and the adherent cells were washed twice with 1× PBS buffer. TFBS solution (0.8 mL, 0.5 μM) was then added to the chamber. After incubation for 2 h, cells were washed three times with 1× PBS buffer. The cells were then imaged with multiphoton microscopes (Leica TCS SP5 X) with a Leica HCX PL APO 63x/1.20 W CORR CS objective lens. The probe was excited with a mode-locked Ti-Sapphire laser source (Chameleon Ultra II) at a wavelength of 800 nm with an output power of ~4 W, which corresponded to an average power of 10 mW in the focal plane. Internal PMTs were used to collect the signals at 500−600 nm in an 8-bit unsigned 1024 × 1024 pixels at a scan speed of 400 Hz.

RESULTS AND DISCUSSION

The synthetic route toward conjugated oligomers TFBN, TFBC, and TFBS is depicted in Scheme 1. 2,7-Dibromo-9,9′-bis(6-bromohexyl)fluorene was synthesized according to our previous reports.[24−28] Coupling 1-amino-2-thiophenol with 4-bromobenzaldehyde in *N*-methyl-2-pyrrolidone (NMP) at 110 °C for 3 days afforded 2-(4-bromophenyl)benzo[d]thiazole (**1**) in 80% yield.[29] **1** was then converted to boronic ester 1-benzothiazole-4-phenylpinacolatoborane (**2**) in 86% yield upon heating with bis(pinacolato)diborane and KOAc in anhydrous dioxane at

dx.doi.org/10.1021/cm201377u |*Chem. Mater.* 2011, 23, 4428–4434

90 °C.[30] Coupling between 1 equiv of **2** and 2,7-dibromo-9,9′-bis(6-bromohexyl)fluorene under Suzuki coupling reaction condition afforded 2-(4-(2-bromo-9,9′-bis(6-bromohexyl)-fluoren-7-yl)phenyl)benzo[d]thiazole (**4**) in 50% yield. Further Suzuki coupling reaction between **4** and 4,4′,4″-tris(pinacolatoborane)-phenylamine (**5**) at a molar ratio of 3.6:1 afforded the desired neutral oligomer (TFBN) in 18% yield. The correct chemical structure of TFBN was affirmed by NMR spectroscopy (see Figure S1 in the Supporting Information) and MALDI-TOF mass spectroscopy. The cationic derivative TFBC was obtained in 86% yield by quaternization of TFBN, using trimethylamine in THF/H_2O.[31] The ^1H NMR spectrum of TFBC shows a single broad peak at 3.02 ppm, which is assigned to the methyl protons in $-CH_2CH_2N(\underline{CH_3})_3$. Integration of the methyl peak area to that of the other alkyl peaks is 9:12, indicating 100% quaternization for TFBN (see Figure S2 in the Supporting Information).

A post-functionalization approach was adopted to synthesize the glucose-substituted oligomer TFBS.[32,33] Coupling TFBN with 1-thio-β-D-glucose tetraacetate at a molar ratio of 1:9 in THF at room temperature afforded acetylated precursor TFBS-OAc in 67% yield. The characteristic single resonance peaks of acetyl protons[34] were observed at 2.01−1.96 ppm in the ^1H NMR spectrum of TFBS-OAc (see Figure S3 in the Supporting Information), indicating successful attachment of acetylated glucose onto TFBN. Moreover, when one compares the NMR spectra between TFBN and TFBS-OAc, the characteristic triplet for protons in $-CH_2Br$ was not observed in the spectrum of TFBS-OAc, indicating 100% replacement of Br by acetylated glucose. After deacetylation of TFBS-OAc in methanol/dichloromethane at room temperature using $NaOCH_3$, the glucose-substituted oligomer TFBS was obtained in 93% yield after dialysis against Mill-Q water using a 3KDa molecular weight cutoff membrane. The disappearance of characteristic peaks of acetyl protons in ^1H NMR spectrum of TFBS (see Figure S4 in the Supporting Information) affirmed complete deacetylation. In addition, the correct molecular mass of TFBS was confirmed by MALDI-TOF mass spectroscopy (see Figure S5 in the Supporting Information).

Scheme 1. Synthetic Route to Oligomers TFBN, TFBC, and TFBS [a]

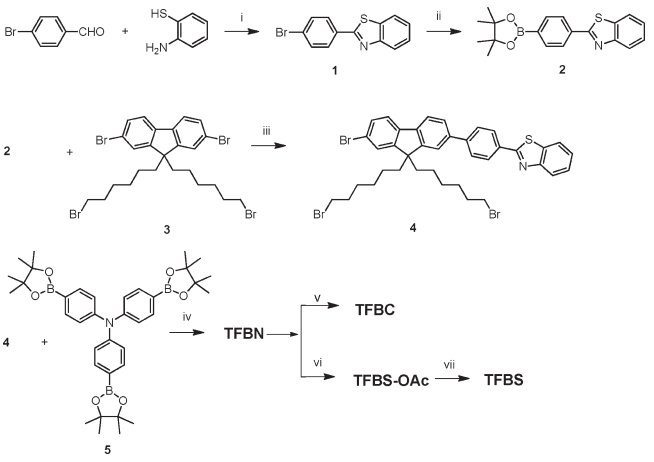

[a] Reagents and conditions: (i) NMP, 110 °C, 3 days; (ii) Bis(pinacolato)-diborane, KOAc, $Pd(dppf)Cl_2$, dioxane, 80 °C, overnight; (iii and iv) Na_2CO_3, $Pd(PPh_3)_4$, toluene/H_2O, 100 °C, overnight; (v) THF/H_2O, NMe_3, 24 h; (vi) 1-thio-β-D-glucose tetraacetate, THF, K_2CO_3, RT, 2 days; and (vii) NaOMe, MeOH/DCM, RT, 12 h.

Dynamic light scattering (DLS) was performed to probe the self-assembly behaviors of TFBC and TFBS in water. Figure 2a shows the DLS spectrum of 2.5 μM TFBS in water. The mean hydrodynamic diameter was measured to be 61 nm, with a polydispersity of 0.29. Similar to the previously reported micellization behaviors of sugar-substituted molecules,[35] the formation of nanoparticles for TFBS is due to the glucose substituents. In contrast, no DLS signal was observed for 2.5 μM TFBC in water, revealing that the cationic oligomer is well-dissolved at the molecular level in solution.[36] Similarly, there was no DLS signal observed for 2.5 μM TFBS and TFBC in DMSO.

The AFM height image and the corresponding cross section analysis of TFBS nanoparticles on silicon wafer are shown in Figures 2b and 2c, respectively. Monolayer spherical nanoparticles are observed with relatively uniform diameter and narrow height distribution. This indicates ordered self-assembly of TFBS in pure water, rather than random aggregation. For all the nanoparticles, an average diameter of 80 nm was determined by statistical analysis and an average central height of 10 nm was obtained by cross-sectional analysis. The smaller size in vertical height is caused by collapse upon transforming the nanoparticles from solution state into dry state, which rationalizes the larger size of nanoparticles measured by AFM, compared to that by DLS.[37] It is expected that the self-assembly of TFBS in aqueous solution would enhance the hydrophobicity of local environment for the star-shaped backbone.

The solvent effect on the optical properties of the neutral oligomer TFBN was investigated. Figure 3 shows the UV−vis absorption and PL spectra of 2 μM TFBN in toluene, dichloromethane (DCM), and dimethylformamide (DMF). With increasing

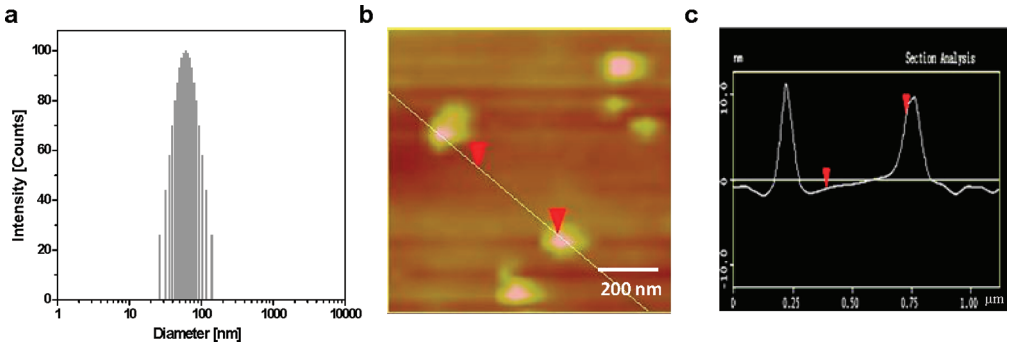

Figure 2. (a) Hydrodynamic diameter of TFBS in water at [TFBS] = 2.5 μM. (b) AFM height image of TFBS nanoparticles. (c) Cross-sectional analysis of TFBS nanoparticles.

dx.doi.org/10.1021/cm201377u |*Chem. Mater.* 2011, 23, 4428–4434

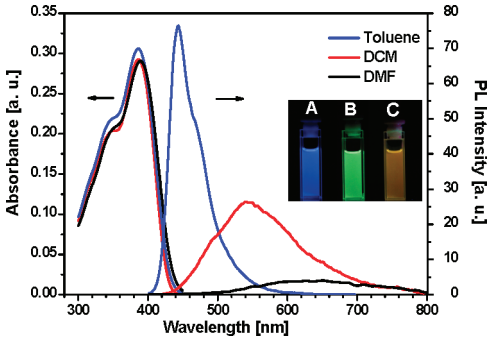

Figure 3. Ultraviolet-visible light (UV−vis) absorption and photoluminescence (PL) spectra of TFBN in toluene, DCM, and DMF at a concentration of 2 μM (excited at λ_{max}). The inset shows the fluorescence from solutions of TFBN in (A) toluene, (B) DCM, and (C) DMF under a hand-held UV lamp with λ_{max} = 365 nm.

solvent polarity, the maximum emission wavelength progressively red-shifts from 440 nm in toluene to 540 nm in DCM and 640 nm in DMF. The solvent-dependent emission maximum originates from the charge transfer character of the excited state of TFBN, which is clearly understood by molecular orbital simulation conducted on a single arm of TFBN. As shown in Figure S6 in the Supporting Information, the highest occupied molecular orbital (HOMO) energy level of the arm is mainly delocalized over the triphenylamine and fluorene units, while the lowest unoccupied molecular orbital (LUMO) is nearly localized on the phenylbenzo[d]thiazole unit. The orbital patterns implicate that the HOMO−LUMO transition for TFBN is accompanied by charge transfer from the electron-donating triphenylamine to the electron-deficient phenylbenzo[d]thiazole unit in the excited state. The quantum yield of TFBN decreases from 0.86 in toluene to 0.69 in DCM and 0.10 in DMF, measured using quinine sulfate in 0.1 M H_2SO_4 as standard. The quenched fluorescence of TFBN with increasing solvent polarity further proves its charge-transfer excited state. As a result of the solvent-dependent emission, the solution fluorescent color of TFBN is blue in toluene, green in DCM, and orange in DMF (see the inset in Figure 3). On the other hand, TFBN has the same absorption spectrum in all solvents, which indicates that the ground state of TFBN is less sensitive to solvent polarity, as both states are exposed to the same local environment.[37]

The UV−vis absorption and PL spectra of TFBC and TFBS in DMSO and pure water are shown in Figure 4. In DMSO, both the absorption and PL spectra of TFBC and TFBS are almost the same. The absorption and emission maxima are observed at 388 and 660 nm, respectively. Moreover, they have a similar quantum yield of 0.09. In water, the absorption maxima for TFBC and TFBS are observed at 384 and 388 nm, while the emission maxima for TFBC and TFBS are observed at 575 and 533 nm, respectively. The quantum yields of TFBC and TFBS in water are 0.03 and 0.10, respectively. Because TFBC and TFBS share the same conjugated framework, both should show decreased fluorescence with increased solvent polarity, because of the charge transfer character of their excited states. The higher quantum yield of TFBS in water agrees with the DLS and AFM results, which show that TFBS self-assembles into nanoparticles in water. The nanoparticles should increase the hydrophobicity in the local environment of TFBS, which leads to the higher quantum yield, relative to that of TFBC.[38] As such, the aqueous

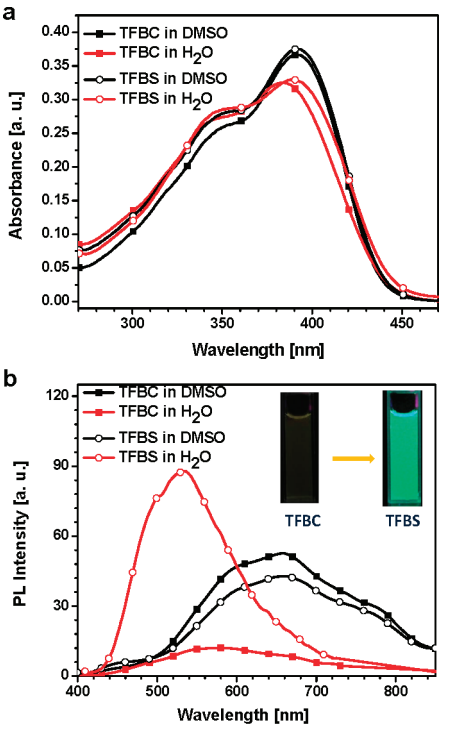

Figure 4. (a) UV−vis absorption spectra and (b) PL spectra of TFBC and TFBS in DMSO and water at a concentration of 2 μM (excited at λ_{max}). The inset in panel (b) shows the fluorescence from solutions of TFBC (left) and TFBS (right) in water under a hand-held UV lamp with λ_{max} = 365 nm.

solution of TFBS shows much brighter fluorescence (see the inset in Figure 4b), making it more suitable for optical applications.

The TPA spectra of TFBN, TFBC, and TFBS were collected using a standard two photon-excited fluorescence (TPEF) technique with a femtosecond pulsed laser source.[39,40] To avoid the interference on TPEF by laser excitation, TPA spectra were measured starting at the wavelength where each individual oligomer has almost no emission. In addition, limited by the laser availability in our experiments, TFBN in toluene was investigated in the range of 640−810 nm; TFBC and TFBS in water were studied in the range of 740−900 nm, and TFBS and TFBC in DMSO were measured in the range of 800−970 nm.

The TPA spectrum of TFBN in toluene shows a maximum TPA cross section (δ_{max}) of 2494 GM at 680 nm (see Figure S7 in the Supporting Information). This value is higher than that for the linear benzothiazole-containing counterparts (<1600 GM).[41−43] On the other hand, compared to AF-350 reported by Tan et al.,[44,45] TFBS has a larger TPA cross section than AF-350 (~500 GM vs 132 GM) at ~790 nm, when both are measured using a femtosecond pulsed laser. The large δ value of TFBN in toluene is mainly ascribed to efficient intramolecular charge transfer (ICT) from the center to peripheries in the octupolar structure. In DMSO, the δ_{max} values of TFBC and TFBS are observed at 800 nm (see Figure S8 in the Supporting Information), which are 435 and 444 GM, respectively. In water, TFBS shows a δ_{max} value of 1195 GM at 740 nm (see Figure 5), while the TPEF spectra for TFBC are barely detectable under the same experimental conditions. Note that the δ value of TFBS in water at 800 nm is 574 GM, which is also larger than that in DMSO (444 GM).

dx.doi.org/10.1021/cm201377u |Chem. Mater. 2011, 23, 4428–4434

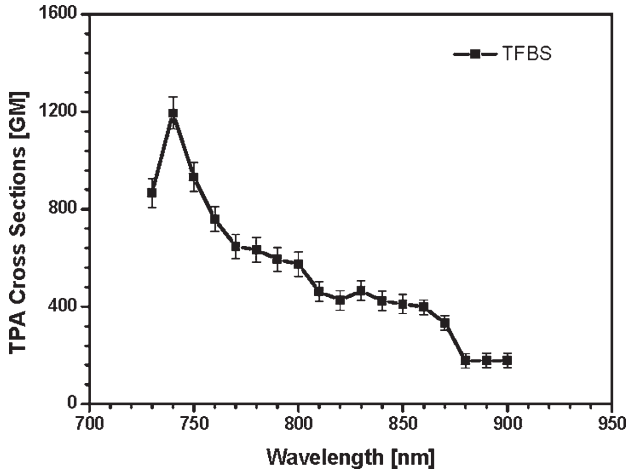

Figure 5. TPA cross sections of TFBS in water.

Because TFBN, TFBC, and TFBS have the same conjugated framework, their TPA values in different solvents should be associated with the solvent effect and molecular assembly. Wang et al.[46] suggested that the enhancement of δ from a solvent of low polarity to that of intermediate polarity is associated with the charge separation assisted by the solvent, and the resulting change in the electronic structure provides a main perturbation on δ. On the other hand, Woo et al. reported that water could influence the electronic structure of D-π-A-π-D chromophores via hydrogen bonding, which led to decreased ICT.[47] As a consequence, a substantial drop in δ was observed in water, compared to that in organic solvents. A similar trend is observed for TFBC, which is well-dissolved at the molecular level in both DMSO and water. However, as TFBS forms self-assembled nanoparticles in water, the star-shaped backbone is isolated within a relatively hydrophobic environment. As such, TFBS shows a significantly higher δ_{max} in water, compared to that for TFBC. This argument is further supported by the comparable δ_{max} values in DMSO for TFBC and TFBS (see Figure S8 in the Supporting Information), because both are well-dissolved at the molecular level. However, the δ_{max} value of TFBS in water is still lower than that for TFBN in toluene, indicating the inevitable loss of TPA when converting TPA molecules from low-polar organic solvents into high-polar aqueous media.

To demonstrate the ability of TFBS as a probe for live cell imaging in vitro, the human cervical cancer cell (Hela cell) line was used as an example. Hela cells were incubated with an aqueous solution of TFBS at a concentration of 0.5 μM for 2 h. After the cell uptake, excess TFBS was washed away and the live cells were imaged using TPM. The excitation wavelength was fixed at 800 nm with a laser power of ~4 W, which corresponded to an average power of 10 mW in the focal plane. The fluorescent signals were collected over the range of 500−600 nm. Note that TFBS has a δ value of ~570 GM at 800 nm in water, which is sufficient to obtain bright TPM images. Moreover, the δ values of TFBS reach up to 1200 GM in the range of 730−800 nm, which are larger than that for many recently reported two-photon fluorescence probes designed for cellular imaging applications.[19−22,48,49] As shown in Figure 6A, the bright green fluorescence indicates successful internalization of TFBS by live Hela cells. As a glucose analogue, TFBS is possibly internalized by Hela cells through a glucose-specific transport system rather than by passive diffusion.[49] The TPEF/transmission overlapped image (Figure 6C) suggests

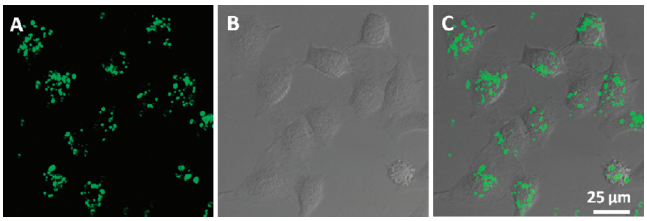

Figure 6. (A) TPEF, (B) transmission, and (C) TPEF/transmission overlapped images of live Hela cells upon incubation with TFBS for 2 h at a concentration of 0.5 μM. Images shown in panels A−C have the same scale bar.

that TFBS is mainly located in the cytoplasm area. To identify its intracellular localization, we costained Hela cells with TFBS and an endosomal tracker (LysoTracker Red).[50] However, the lack of overlap between LysoTracker Red and TFBS indicates that TFBS randomly accumulates throughout cytosol (see Figure S9 in the Supporting Information). Further work on costaining cells with TFBS and other vesicular specific antibodies would be needed to identify the accurate TFBS localization.

The cytotoxicity of TFBS was evaluated for mouse embryonic fibroblast normal cells (NIH-3T3), using methylthiazolyldiphenyl-tetrazolium (MTT) cell viability assay. Figure S10 in the Supporting Information shows the in vitro NIH-3T3 cell viabilities after being cultured with aqueous TFBS solution at the concentrations of 0.5 and 1 μM for 24, 48, and 72 h, respectively. The cell viabilities are close to 100% within the tested period of time, which indicates low cytotoxicity of TFBS. This low cytotoxicity would benefit TFBS for in vitro and in vivo cellular imaging and other clinical applications.

CONCLUSION

In conclusion, we have synthesized a glycosylated star-shaped neutral conjugated oligomer (4,4′,4″-tris(4-(2-(4-(benzo[d]thiazol-2-yl)phenyl)-9,9′-bis(6-thiol-β-D-glucose)-hexyl)-fluoren-7-yl)-phenylamine (TFBS)), using a post-functionalization strategy for two-photon fluorescence imaging of live cells. Because of the presence of hydrophilic glucose substituents, TFBS is able to self-assemble into nanoparticles in aqueous media. The nanoparticles show a high two-photon absorption (TPA) cross section of ~1200 GM at 740 nm in water, which is higher than that for recently reported water-soluble TPA chromophores for two-photon microscopy (TPM) applications. In contrast, the TPA spectrum for its cationic counterpart (4,4′,4″-tris(4-(2-(4-(benzo-[d]thiazol-2-yl)phenyl)-9,9′-bis(6-*N*,*N*,*N*-trimethylammonium)-hexyl)-fluoren-7-yl)phenylamine (TFBC)) is not measurable using TPEF method, because of its extremely low fluorescence in water, which highlights the importance of glucose substitution in achieving high TPA action cross-section in water. Moreover, TFBS has low cytotoxicity and efficient permeability to live cells, which makes it an ideal probe for two-photon fluorescence imaging of live cells in a high-contrast and nonviral manner. This study thus demonstrates an effective molecular engineering strategy to develop robust water-soluble TPA materials for TPM applications.

ASSOCIATED CONTENT

Supporting Information. TPA measurement, ^{1}H NMR of TFBN, TFBC, TFBS-OAc and TFBS, MALDI-TOF mass

dx.doi.org/10.1021/cm201377u |*Chem. Mater.* 2011, 23, 4428–4434

spectrum of TFBS, density functional theory (DFT) calculation, TPA cross sections of TFBN in toluene as well as TFBS and TFBC in DMSO, and cell viability of NIH-3T3 fibroblast cells after incubation with TFBS. This material is available free of charge via the Internet at http://pubs.acs.org.

AUTHOR INFORMATION

Corresponding Author

*Fax: (+65) 6779-1936 (B.L.). E-mails: cheliub@nus.edu.sg, (B.L.), chmlaiyh@nus.edu.sg (Y.-H.L.).

ACKNOWLEDGMENT

The authors are grateful to the Singapore National Research Foundation (R279-000-323-281), the Temasek Defence Systems Institute (R279-000-305-232/422/592), and the Institute of Materials Research Engineering (IMRE/11-1C0213) for financial support.

REFERENCES

(1) Albota, M.; Beljonne, D.; Brédas, J.; Ehrlich, J. E.; Fu, J.; Heikal, A. A.; Hess, S.; Kogej, T.; Levin, M. D.; Marder, S. R.; McCord-Maughon, D.; Perry, J. W.; Röckel, H.; Rumi, M.; Subramaniam, G.; Webb, W.; Wu, X.; Xu, C. *Science* **1998**, *281*, 1653.

(2) Cumpston, B. H.; Ananthavel, S. P.; Barlow, S.; Dyer, D. L.; Ehrlich, J. E.; Erskine, L. L.; Heikal, A. A.; Kuebler, S. M.; Lee, I. L. S.; McCord-Maughon, D.; Qin, J.; Röckel, H.; Rumi, M.; Wu, X.; Marder, S. R.; Perry, J. W. *Nature* **1999**, *389*, 51.

(3) Pawlicki, M.; Collins, H. A.; Denning, R. G.; Anderson, H. L. *Angew. Chem., Int. Ed.* **2009**, *48*, 3244.

(4) Denk, W.; Strickler, J. H.; Webb, W. W. *Science* **1990**, *248*, 73.

(5) Xu, C.; Zipfel, W.; Shear, J. B.; Williams, R. M.; Webb, W. W. *Proc. Natl. Acad. Sci. U.S.A.* **1996**, *93*, 10763.

(6) So, P. T. C.; Dong, C. Y.; Masters, B. R.; Berland, K. M. *Annu. Rev. Biomed. Eng.* **2000**, *2*, 399.

(7) Le Droumaguet, C.; Mongin, O.; Werts, M. H. V.; Blanchard-Desce, M. *Chem. Commun.* **2005**, 2802.

(8) Mongin, O.; Porrès, L.; Katan, C.; Mertzb, T. P. J.; Blanchard-Descea, M. *Tetra. Lett.* **2003**, *44*, 8121.

(9) Yoo, J.; Yang, S. K.; Jeong, M.-Y.; Ahn, H. C.; Jeon, S.-J.; Cho, B. R. *Org. Lett.* **2003**, *5*, 645.

(10) Cui, Y.-Z.; Fang, Q.; Xue, G.; Xu, G.-B.; Yin, L.; Yu, W.-T. *Chem. Lett.* **2005**, *34*, 644.

(11) Cho, B. R.; Son, K. H.; Lee, S. H.; Song, Y.-S.; Lee, Y.-K.; Jeon, S.-J.; Choi, J. H.; Lee, H.; Cho, M. *J. Am. Chem. Soc.* **2001**, *123*, 10039.

(12) Tian, Y.; Chen, C.-Y.; Cheng, Y.-J.; Young, A. C.; Tucker, N. M.; Jen, A. K.-Y. *Adv. Funct. Mater.* **2007**, *17*, 1691.

(13) Woo, H. Y.; Korystov, D.; Mikhailovsky, A.; Nguyen, T.-Q.; Bazan, G. C. *J. Am. Chem. Soc.* **2005**, *127*, 13794.

(14) Jager, W. F.; Volkers, A. A.; Neckers, D. C. *Macromolecules* **1995**, *28*, 8153.

(15) Stubenrauch, C. *Curr. Opin. Colloid Interface Sci.* **2001**, *6*, 160.

(16) Koo, C.-K.; Wong, K.-L.; Man, C. W.-Y.; Lam, Y.-W.; So, L. K.-Y.; Tam, H.-L.; Tsao, S.-W.; Cheah, K.-W.; Lau, K.-C.; Yang, Y.-Y.; Chen, J.-C.; Lam, M. H.-W. *Inorg. Chem.* **2009**, *48*, 878.

(17) Koo, C.-K.; Wong, K.-L.; Man, C. W.-Y.; Tam, H.-L.; Tsao, S.-W.; Cheah, K.-W.; Lam, M. H.-W. *Inorg. Chem.* **2009**, *48*, 7501.

(18) Koo, C.-K.; So, L. K.-Y.; Wong, K.-L.; Ho, Y.-M.; Lam, Y.-W.; Lam, M. H.-W.; Cheah, K.-W.; Cheng, C. C.-W.; Kwok, W.-M. *Chem.—Eur. J.* **2010**, *16*, 3942.

(19) Ohulchanskyy, T. Y.; Pudavar1, H. E.; Yarmoluk, S. M.; Yashchuk, V. M.; Bergey, E. J.; Prasad, P. N. *Photochem. Photobiol.* **2003**, *77*, 138.

(20) Dyrager, C.; Friberg, A.; Dahlén, K.; Fridén-Saxin, M.; Börjesson, K.; Wilhelmsson, L. M.; Smedh, M.; Grøtli, M.; Luthman, K. *Chem.—Eur. J.* **2009**, *15*, 9417.

(21) McRae, R. L.; Phillips, R. L.; Kim, I.-B.; Bunz, U. H. F.; Fahrni, C. J. *J. Am. Chem. Soc.* **2008**, *130*, 7851.

(22) Warther, D.; Bolze, F.; Léonard, J.; Gug, S.; Specht, A.; Puliti, D.; Sun, X.-H.; Kessler, P.; Lutz, Y.; Vonesch, J.-L.; Winsor, B.; Nicoud, J.-F.; Goeldner, M. *J. Am. Chem. Soc.* **2010**, *132*, 2585.

(23) Jiang, Y.; Wang, Y.; Wang, B.; Yang, J.; He, N.; Qian, S.; Hua, J. *Chem. Asian J.* **2011**, *6*, 157.

(24) Liu, B.; Gaylord, B. S.; Wang, S.; Bazan, G. C. *J. Am. Chem. Soc.* **2003**, *125*, 6705.

(25) Liu, B.; Wang, S.; Bazan, G. C.; Mikhailovsky, A. *J. Am. Chem. Soc.* **2003**, *125*, 13306.

(26) Liu, B.; Bazan, G. C. *J. Am. Chem. Soc.* **2006**, *128*, 1188.

(27) Liu, B.; Bazan, G. C. *Chem. Asian J.* **2007**, *2*, 499.

(28) Liu, B.; Bazan, G. C. *J. Am. Chem. Soc.* **2004**, *126*, 1942.

(29) Lin, T.-C.; He, G. S.; Prasad, P. N.; Tan, L.-S. *J. Mater. Chem.* **2004**, *14*, 982.

(30) Pu, K.-Y.; Fang, Z.; Liu, B. *Adv. Funct. Mater.* **2008**, *18*, 1321.

(31) Pu, K. Y.; Pan, S. Y. H.; Liu, B. *J. Phys. Chem. B* **2008**, *112*, 9295.

(32) Xue, C.; Jog, S. P.; Murthy, P.; Liu, H. *Biomacromolecules* **2006**, *7*, 2470.

(33) Xue, C.; Donuru, V. R. R.; Liu, H. *Macromolecules* **2006**, *39*, 5747.

(34) Pu, K.-Y.; Shi, J.; Wang, L.; Cai, L.; Wang, G.; Liu, B. *Macromolecules* **2010**, *43*, 9690.

(35) Eastoe, J.; Rogueda, P.; Harrison, B. J.; Howe, A. M.; Pitt, A. R. *Langmuir* **1994**, *12*, 4429.

(36) Chu, B. *Laser Light Scattering: Basic Principles and Practice*, 2nd ed.; Academic Press: San Diego, CA, 1991.

(37) Pu, K.-Y.; Li, K.; Liu, B. *Adv. Funct. Mater.* **2010**, *20*, 2770.

(38) Pu, K.-Y.; Liu, B. *Adv. Funct. Mater.* **2009**, *19*, 277.

(39) Xu, C.; Webb, W. W. *J. Opt. Soc. Am. B* **1996**, *13*, 481.

(40) Makarov, N. S.; Drobizhev, M.; Rebane, A. *Opt. Express* **2008**, *16*, 4029.

(41) Hrobarikova, V.; Hrobarik, P.; Gajdos, P.; Fitilis, I.; Fakis, M.; Persephonis, P.; Zahradnik, P. *J. Org. Chem.* **2010**, *75*, 3053.

(42) Yao, S.; Ahn, H.-Y.; Wang, X.; Fu, J.; Van Stryland, E. W.; Hagan, D. J.; Belfield, K. D. *J. Org. Chem.* **2010**, *75*, 3965.

(43) Andrade, C. D.; Yanez, C. O.; Rodriguez, L.; Belfield, K. D. *J. Org. Chem.* **2010**, *75*, 3975.

(44) He, G. S.; Swiatkiewicz, J.; Jiang, J.; Prasad, P. N.; Reinhardt, B. A.; Tan, L.-S.; Kannan, R. *J. Phys. Chem. A* **2000**, *104*, 4805.

(45) Kannan, R.; He, G. S.; Lin, T.-C.; Prasad, P. N.; Vaia, R. A.; Tan, L.-S. *Chem. Mater.* **2004**, *16*, 185.

(46) Wang, C.-K.; Zhao, K.; Su, Y.; Ren, Y.; Zhao, X.; Luo, Y. *J. Chem. Phys.* **2003**, *119*, 1208.

(47) Woo, H. Y.; Liu, B.; Kohler, B.; Korystov, D.; Mikhailovsky, A.; Bazan, G. C. *J. Am. Chem. Soc.* **2005**, *127*, 14721.

(48) Morales, A. R.; Luchita, G.; Yanez, C. O.; Bondar, M. V.; Przhonskab, O. V.; Belfield, K. D. *Org. Biomol. Chem.* **2010**, *8*, 2600.

(49) Tian, Y. S.; Lee, H. Y.; Lim, C. S.; Park, J.; Kim, H. M.; Shin, Y. N.; Kim, E. S.; Jeon, H. J.; Park, S. B.; Cho, B. R. *Angew. Chem., Int. Ed.* **2009**, *48*, 8027.

(50) Khan, S.; Bijker, M. S.; Weterings, J. J.; Tanke, H. J.; Adema, G. J.; van Hall, T.; Drijfhout, J. W.; Melief, C. J. M.; Overkleeft, H. S.; van der Marel, G. A.; Filippov, D. V.; van der Burg, S. H.; Ossend, F. *J. Biol. Chem.* **2007**, *282*, 21145.